Mitochondrial Nuclear Retrograde Regulator 1 (MNRR1) rescues the cellular phenotype of MELAS by inducing homeostatic mechanisms

Siddhesh Aras[a], Neeraja Purandare[a], Stephanie Gladyck[a], Mallika Somayajulu-Nitu[a], Kezhong Zhang[a], Douglas C. Wallace[b,c,1], and Lawrence I. Grossman[a,1]

[a]Center for Molecular Medicine and Genetics, Wayne State University School of Medicine, Detroit, MI 48201; [b]Center for Mitochondrial and Epigenomic Medicine, Children's Hospital of Philadelphia Research Institute, Philadelphia, PA 19104; and [c]Department of Pediatrics, Division of Human Genetics, The Children's Hospital of Philadelphia, Perelman School of Medicine, University of Pennsylvania, Philadelphia, PA 19104

Contributed by Douglas C. Wallace, October 20, 2020 (sent for review March 30, 2020; reviewed by Agnieszka Chacinska, Chih-Hao Lee, and Keshav K. Singh)

MNRR1 (CHCHD2) is a bi-organellar regulator of mitochondrial function that directly activates cytochrome *c* oxidase in the mitochondria and functions in the nucleus as a transcriptional activator for hundreds of genes. Since MNRR1 depletion contains features of a mitochondrial disease phenotype, we evaluated the effects of forced expression of MNRR1 on the mitochondrial disease MELAS (mitochondrial encephalomyopathy, lactic acidosis and stroke-like episodes) syndrome. MELAS is a multisystem encephalomyopathy disorder that can result from a heteroplasmic mutation in the mitochondrial DNA (mtDNA; m.3243A > G) at heteroplasmy levels of ∼50 to 90%. Since cybrid cell lines with 73% m.3243A > G heteroplasmy (DW7) display a significant reduction in MNRR1 levels compared to the wild type (0% heteroplasmy) (CL9), we evaluated the effects of MNRR1 levels on mitochondrial functioning. Overexpression of MNRR1 in DW7 cells induces the mitochondrial unfolded protein response (UPR^{mt}), autophagy, and mitochondrial biogenesis, thereby rescuing the mitochondrial phenotype. It does so primarily as a transcription activator, revealing this function to be a potential therapeutic target. The role of MNRR1 in stimulating UPR^{mt}, which is blunted in MELAS cells, was surprising and further investigation uncovered that under conditions of stress the import of MNRR1 into the mitochondria was blocked, allowing the protein to accumulate in the nucleus to enhance its transcription function. In the mammalian system, ATF5, has been identified as a mediator of UPR^{mt}. MNRR1 knockout cells display an ∼40% reduction in the protein levels of ATF5, suggesting that MNRR1 plays an important role upstream of this known mediator of UPR^{mt}.

CHCHD2 | mitochondria | transcription | unfolded protein response | cytochrome c oxidase

MNRR1 (CHCHD2) is a bi-organellar regulator of mitochondrial function. In the mitochondria, MNRR1 binds to cytochrome *c* oxidase (COX) and activates respiration (1, 2). In the nucleus, MNRR1 functions to activate transcription by binding to the conserved oxygen-responsive promoter element (ORE) of a number of genes that are part of stress-responsive pathways and also to its own promoter (2, 3). Furthermore, MNRR1 has also been shown to function as an antiapoptotic protein via its interaction with Bcl-xL (4).

In examining the function of MNRR1, we observed that at the cellular level, depletion of MNRR1 produced a phenocopy of many mitochondrial diseases, such as reduced respiration and ATP production, along with increased glycolysis, reactive oxygen species (ROS) production, and lactic acidosis. To evaluate the role of MNRR1 in a well-studied mitochondrial disease, we chose a MELAS (mitochondrial encephalomyopathy, lactic acidosis and stroke-like episodes) model. MELAS is a multisystem disorder commonly caused by mutations in the mitochondrial DNA (mtDNA). Several mtDNA mutations have been reported to cause MELAS, including *MT-ND1* (5), *MT-ND5* (6), *MT-TH* (7), *MT-TL1* (8), and *MT-TV* (9). The MT-TL1 ($tRNA^{Leu(UUR)}$ m.3243A > G) mutation (10) is the most common mtDNA mutation associated with the MELAS phenotype. It perturbs mitochondrial protein synthesis and causes MELAS at heteroplasmy levels generally >50%. This same m.3243A > G mtDNA mutation at >90% can result in the fatal Leigh syndrome, and at ≤30% can present as diabetes or autism (11).

Mitochondria not only generate energy, but are also involved as a platform in key cellular pathways, such as metabolic signaling and apoptosis. Thus, mitochondrial function is finely regulated under conditions of stress to maintain cellular homeostasis. The endoplasmic reticulum (ER) is responsible for optimal folding and quality control of many proteins in a cell; however, on ER stress, this process is interrupted, causing an accumulation of unfolded or misfolded proteins in the ER and setting into action a cascade of events termed the unfolded protein response (UPR) (12). The main goal of the UPR is to achieve physiological homeostasis by inducing chaperones or folding enzymes that increase protein folding capability, activating salvage pathways such as autophagy, detoxifying ROS, and enhancing mitochondrial function to generate the ATP required

Significance

Pathogenic mtDNA tRNA mutations, such as the 3243A>G MELAS mutation, generally result in multisystem failure. In cybrids harboring ∼70% 3243G mutant mtDNA, the mitochondrial unfolded protein response (UPR^{mt}) is impaired. Mitochondrial Nuclear Retrograde Regulator 1 (MNRR1, or CHCHD2) is a bi-organellar (mitochondrial and nuclear) protein that is reduced in ∼70% 3243G cybrid cells. Under stress conditions, MNRR1 import into mitochondria is impaired, resulting in its preferential concentration in the nucleus. Increased nuclear MNRR1 induces the UPR^{mt} through regulation of the ATF5 transcription factor. Overexpression of MNRR1 in ∼70% 3243G cybrid cells induces the UPR^{mt}, autophagy, and mitochondrial biogenesis and restores mitochondrial respiratory function; furthermore, the proportion of wild-type mtDNA increases. Thus, MNRR1 overexpression might be beneficial for mtDNA diseases.

Author contributions: S.A., D.C.W., and L.I.G. designed research; S.A., N.P., S.G., M.S.-N., and K.Z. performed research; D.C.W. contributed new reagents/analytic tools; S.A., N.P., S.G., M.S.-N., K.Z., and L.I.G. analyzed data; S.A. and L.I.G. wrote the paper.

Reviewers: A.C., University of Warsaw; C.-H.L., Harvard School of Public Health; and K.K.S., University of Alabama at Birmingham.

Competing interest statement: Company associations for D.C.W. not related to the manuscript include MitoCURia, Mitrios, and Panos.

[1]To whom correspondence may be addressed. Email: WallaceD1@email.chop.edu or lgrossman@wayne.edu.

This article contains supporting information online at https://www.pnas.org/lookup/suppl/doi:10.1073/pnas.2005877117/-/DCSupplemental.

First published November 30, 2020.

(13), although chronic activation of the UPR stimulates cells to undergo apoptosis (14). At least three major UPR pathways become activated in response to ER stress, which are mediated by the ER-transmembrane proteins IRE1, ATF6, and PERK (reviewed in ref. 15). In addition, cAMP response element-binding protein transcription factor, hepatic-specific (CREBH), a liver-enriched ER-resident transcription factor, is activated in response to ER stress, inflammatory stimuli, or circadian cues (16, 17). It has been shown that activated CREBH functions as a potent transcriptional regulator to maintain hepatic lipid and glucose homeostasis under stress conditions (17, 18).

Mitochondria contain a pathway similar to the ER UPR (UPR^{ER}) termed the mitochondrial UPR (UPR^{mt}) (19, 20). Since mitochondria are critical for cellular health, it is not surprising that they also contain a UPR pathway to help achieve homeostasis in response to stress. The mitochondrial pathway also induces chaperones such as HSP60 (20) and proteases such as YME1L1 (21) that effect proper folding of and aid degradation of misfolded proteins, respectively. In addition to its stress response function, UPR^{mt} also plays key roles in the mitochondrial longevity pathway (22), immune responses to invading pathogens (23), and neurodegenerative phenotypes (24). ATFS-1 in *Caenorhabditis elegans* and ATF5 in mammals have been shown to be the key mediators of UPR^{mt} (25, 26). Much of what is currently known about the UPR^{mt} pathway has been identified using ATFS-1. On stress, ATFS-1 translocates to the nucleus to function as a transcription factor for the UPR^{mt}-responsive genes (26).

In this study, we sought to identify the effect of MNRR1's action on the mitochondrial dysfunction found in a human cybrid cell line harboring an ∼73% m.3243A > G mutation, a heteroplasmy level that commonly presents as MELAS. Thus, in this paper, we refer to cells with an m.3243A > G heteroplasmy level >50% as "MELAS" cells. We show that MNRR1 levels are reduced in MELAS cybrid cells, and that forced expression of MNRR1 in these cybrids rescues the cellular phenotype. Unexpectedly, we also find that MNRR1 is required for activation of UPR^{mt}, which is blunted in 73% m.3243A > G MELAS cybrids. We propose that MNRR1 mediated rescue involves activation of at least three pathways: UPR^{mt}, autophagy, and mitochondrial activation and biogenesis. In addition, MNRR1 also rescues mitochondrial oxygen consumption in cells harboring the mtDNA m.8993T > G mutation causing NARP (neuropathy, ataxia, and retinitis pigmentosa), suggesting MNRR1 as a potential target for multiple mtDNA mutation disorders.

Results

MELAS Cells, 73% m.3243A > G, Have Lower Levels of MNRR1, and Their Defective Mitochondrial Function Is Rescued on Expression of MNRR1. Our characterization of the role of MNRR1 in mitochondrial function suggests that $MNRR1^{-/-}$ cells have a phenotype mimicking that of mitochondrial disease (1, 2, 27). We thus asked whether MNRR1 levels would be lower in a known mitochondrial disease model. To do so, we used the well-characterized cellular model harboring the m.3243A > G mutation at the MELAS heteroplasmy level of 73% (DW7 cybrid) (11) and found that protein and transcript levels of MNRR1 indeed were lower in the DW7 cybrid cells compared with control CL9 (0% m.3243A > G mutation) cells (Fig. 1*A*). In addition, the levels of electron transport chain (ETC) complexes were also lower in the 73% MELAS cybrids (Fig. 1*A*). ETC levels were even lower in cells harboring 100% mutant m.3243A > G mtDNA (DW10) (*SI Appendix*, Fig. S1*A*).

Action by a bi-organellar regulator such as MNRR1 raises the question of whether it is acting via the nucleus, the mitochondria, or both organelles. To address this question, we developed MNRR1 versions that favor one or the other compartment. Phosphomimetic (Y99E) MNRR1 is superior in stimulating respiration (1, 27) but is inhibited as a transactivator in the nucleus (*SI Appendix*, Fig. S1*B*). C-S MNRR1 (all cysteines converted to serine) cannot enter the mitochondria but functions normally in the nucleus (2). Nonacetylatable K-R MNRR1 (all three lysine residues replaced by arginine) is a superior transactivator (*SI Appendix*, Fig. S1*C*), specifically at position 119 (*SI Appendix*, Fig. S1*D*), since acetylation of the other lysines does not affect transactivation (*SI Appendix*, Fig. S1*D*). Acetylation appears to be an in vivo regulatory mechanism, since MNRR1 is a target of SIRT1-induced deacetylation (*SI Appendix*, Fig. S1*E*), and SRT1720, a SIRT1 agonist (28), increases transactivator ability (*SI Appendix*, Fig. S1*F*). SIRT1 has also been shown to interact with MNRR1 (29).

To examine the effect of these reduced ETC levels on mitochondrial respiration, we measured oxygen consumption and found reductions to ∼15% in DW10 cells (*SI Appendix*, Fig. S2*A*) and ∼50% in DW7 cells (Fig. 1*B*) compared with the CL9 0% m.3243A > G cells expressing an empty vector (EV). We then asked whether ectopically increasing levels of MNRR1 would increase mitochondrial respiration. As shown in both DW7 cells (Fig. 1*B*) and DW10 cells (*SI Appendix*, Fig. S2*A*), forced expression of MNRR1 increased oxygen consumption by ∼50% in each case. Expressing the transcriptionally more active K-R mutant (*SI Appendix*, Fig. S1*C*) or the mitochondrially more active Y99E mutant (1) completely rescued mitochondrial oxygen consumption in DW7 cells, superior even to the levels observed with the control CL9 cells (Fig. 1*B*). Consistently, MNRR1-expressing DW7 cells also displayed a reduction in ECAR levels along with the increased oxygen consumption rate (OCR) (*SI Appendix*, Fig. S2*B*). Furthermore, expression of MNRR1 in DW7 cells increased cellular levels of ATP (Fig. 1*C*) and decreased total cellular ROS levels (Fig. 1*D*). Expression of the WT and Y99E mutants enhanced oxygen consumption even in DW10 cells (*SI Appendix*, Fig. S2*A*). Finally, we could visualize the increased function of DW7 mitochondria resulting from MNRR1 expression by following increased protein import, which was shown to be reduced in defective mitochondria (30). To do so, we cotransfected mito-mCherry plus either the EV or WT MNRR1 and then live-stained with MitoTracker Green, which stains all mitochondria. Using confocal microscopy, we could see the overlap of mCherry (31) and MitoTracker Green and observed that mitochondrial import of mCherry was noticeably higher in MNRR1-expressing cells (Fig. 1*E*). To test the generality of MNRR1's ability to rescue mitochondrial respiration in MELAS cells, we examined cells containing the NARP mutation (m.8993T > G) and found reduced MNRR1 amounts and reduced oxygen consumption that could be rescued by MNRR1 expression (*SI Appendix*, Fig. S2*C*).

MELAS Cells Show a Blunted Mitochondrial UPR (UPR^{mt}) that Is Rescued by MNRR1 Expression. Because the UPR^{mt} is expected to be activated by mitochondrial dysfunction, we examined the function of the UPR^{mt} in DW7 MELAS cells. Using YME1L1 as a readout for UPR^{mt} (21), we observed that the ability of doxycycline to induce the UPR^{mt} in DW7 cells is blunted (Fig. 1*F*) and can be rescued by expression of WT MNRR1 (Fig. 1*G*) or its transcriptionally more active mutant. The ability of MNRR1 to restore UPR^{mt} led us to further investigate the role of MNRR1, and we discovered that MNRR1 is required to trigger UPR^{mt}.

Since the ORE element associated with MNRR1-stimulated genes is present in the promoter of YME1L1 and appears to be functional based on increased YME1L1 protein levels at the 4% oxygen tension at which MNRR1 levels peak (2, 3) (*SI Appendix*, Fig. S2*D*), we hypothesized that MNRR1 is linked to the UPR^{mt} response. To test this hypothesis, we examined the protein levels of key UPR^{mt} markers in $MNRR1^{-/-}$ ($R1^{-/-}$) cells. The levels of the two key proteases, YME1L1 and LONP1, as well as

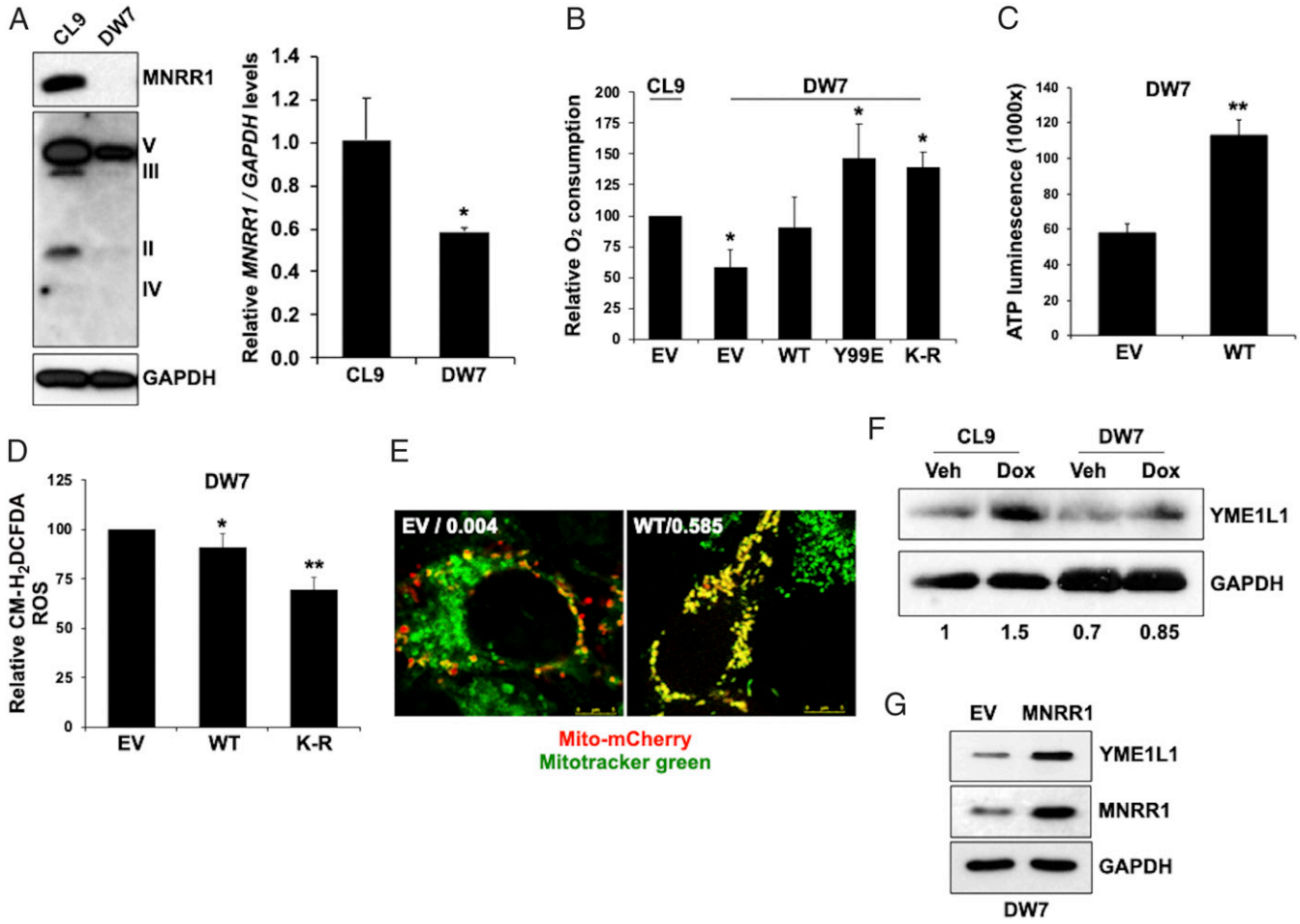

Fig. 1. MNRR1 expression in the deficient MELAS cells rescues mitochondrial function. (*A*) MNRR1 and mitochondrial ETC complex levels in CL9 (100% WT mtDNA) and DW7 (73% mutant mtDNA) MELAS cybrid cells. GAPDH served as a loading control. MNRR1 transcript levels in CL9 and DW7 cells normalized to GAPDH are also shown. (*B*) Intact cellular oxygen consumption in the DW7 MELAS cell lines expressing an EV, WT MNRR1, or the mitochondrially active (Y99E) and transcriptionally active (K-R) mutants of MNRR1. Data are represented as oxygen consumption relative to CL9 cells expressing the EV set to 100%. (*C*) ATP levels in DW7 cells expressing either an EV or WT MNRR1. (*D*) Total cellular ROS levels in DW7 cells expressing an EV, WT MNRR1, or the transcriptionally active mutant (K-R). (*E*) Immunofluorescence microscopy in DW7 cells expressing an EV or WT MNRR1, each along with Mito-mCherry and stained with MitoTracker Green. The Pearson correlation coefficient for yellow overlap intensity is also shown. (*F*) DW7 MELAS cells are defective for their ability to induce UPR^{mt}. CL9 (100% WT mtDNA) and DW7 (73% mutant mtDNA) MELAS cells were treated with either vehicle (Veh) or doxycycline (Dox; 50 μg/mL), and YME1L1 levels were determined. Relative MNRR1 band density is shown beneath. GAPDH served as a loading control. (*G*) MNRR1-expressing DW7 cells show an increase in the YME1L1 protein levels compared with cells expressing an EV. GAPDH served as a loading control.

chaperone HSP60, were reduced in comparison to R1$^{+/+}$ cells (Fig. 2*A*). Furthermore, R1$^{-/-}$ cells were deficient in their ability to induce UPR^{mt} in response to treatment with doxycycline, a known inducer (32), whereas R1$^{+/+}$ cells treated with doxycycline induced YME1L1 (Fig. 1*F*) and HSP60 (Fig. 2*B*). UPR^{mt} can also be induced by expressing a deletion mutant of ornithine transcarbamylase (ΔOTC) that causes protein aggregation in the mitochondrial matrix (20).

To test whether MNRR1 is required for the induction of chaperones and proteases in response to protein misfolding stress, we expressed full-length OTC and ΔOTC in R1$^{+/+}$ and R1$^{-/-}$ cells. We found that ΔOTC-expressing R1$^{+/+}$ control cells displayed an increase in the levels of HSP60 and YME1L1, whereas the R1$^{-/-}$ KO cells did not (Fig. 2*C*), supporting a critical role for MNRR1 in the induction of a UPR^{mt} response. In addition, ATF5, the mammalian effector of UPR^{mt} (25) and a homolog of worm ATFS-1 (26), was reduced in R1$^{-/-}$ cells, suggesting that MNRR1 is upstream of ATF5 (Fig. 2*D*). Finally, to examine whether chemical inducers of UPR^{mt} activate the MNRR1 promoter, we performed MNRR1-promoter luciferase reporter assays. Doxycycline (33) and paraquat (34) both induced the MNRR1 reporter, by ∼2.75-fold and 1.75-fold, respectively (Fig. 2*E*).

We next analyzed the levels of cellular autophagy markers. We found increased levels of ATG7 and Parkin, but decreased p62 and LC3-I/II ratio, on expression of WT MNRR1 in DW7 cells (Fig. 2*F*). The protein signature observed favors the induction of enhanced autophagic flux on MNRR1 expression, which may play a role in the rescue of damaged mitochondria.

UPR^{mt} Is Linked to the ER-UPR. Increasing evidence has linked UPR^{mt} signaling to the widely studied ER-UPR (35). ER stress triggers regulated intramembrane proteolysis by activating downstream transcriptional programs for the induction of cellular stress-responsive genes (36). We observed that chemical inducers of cellular ER stress response, such as brefeldin A, thapsigargin, and tunicamycin, also activate the MNRR1 reporter (Fig. 2*G*), suggesting that MNRR1 is transcriptionally up-regulated whenever a cell is under ER stress. MNRR1 protein levels are also increased, as shown for cells treated with tunicamycin (Fig. 2 *H*,

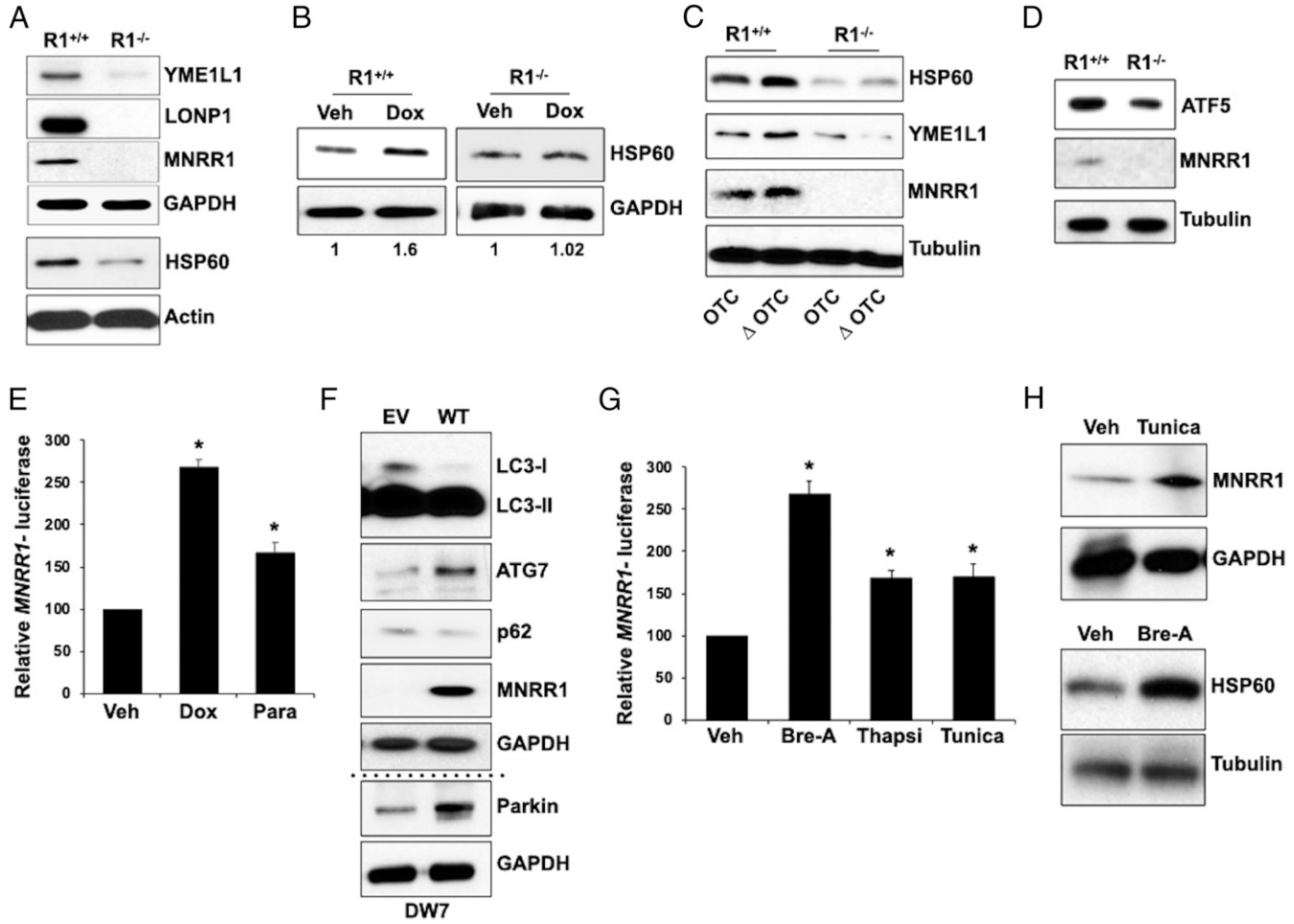

Fig. 2. Cellular stress activates MNRR1, which is required for optimal induction of UPR^{mt}. (*A*) Protein levels of key UPR^{mt} markers in MNRR1-KO HEK 293 cells (R1$^{-/-}$) compared with control cells (R1$^{+/+}$). GAPDH and actin served as loading controls. (*B*) Induction of UPR^{mt} is deficient in MNRR1-KO cells (R1$^{-/-}$) on doxycycline treatment (50 μg/mL) for 48 h. The ratio of HSP60/GAPDH intensity is shown beneath. (*C*) Induction of UPR^{mt} is deficient in MNRR1-KO cells (R1$^{-/-}$) when the deletion mutant of ornithine transcarbamylase (ΔOTC), but not of WT (OTC), is expressed. HSP60 and YME1L1 are probed as markers of UPR^{mt} with tubulin as a loading control. (*D*) ATF5 levels in MNRR1-KO HEK 293 cells (R1$^{-/-}$) compared with control cells (R1$^{+/+}$). Tubulin served as a loading control. (*E*) Dual luciferase assay in HEK 293 cells expressing the MNRR1-luciferase reporter treated with UPR^{mt} inducers doxycycline (50 μg/mL) and paraquat (10 μM) for 48 h. Data are presented relative to cells treated with vehicle. (*F*) Levels of autophagy markers in DW7 MELAS cells expressing either an EV or WT MNRR1. GAPDH served as a loading control. MNRR1 expression was detected by a Flag antibody. (*G*) Dual luciferase assay in cells expressing the MNRR1-luciferase reporter treated with ER stress inducer brefeldin A (Bre-A) (100 μg/mL), thapsigargin (1 μM), or tunicamycin (5 μg/mL). Data are represented relative to cells treated with vehicle. (*H*) MNRR1 protein levels in cells treated with 5 μg/mL tunicamycin (Tunica), with GAPDH as a loading control, and UPR^{mt} marker (HSP60) levels in cells treated with Bre-A (100 μg/mL), a chemical inducer of ER stress, with tubulin as a loading control.

Upper). Importantly, activating the cellular ER stress response also induces UPR^{mt} (Fig. 2 *H*, *Lower*).

CREBH, originally identified as liver-specific (16), is an ER-resident protein that, in conjunction with ATF6 or PPARα, mediates a pathophysiological UPR that is functionally involved in acute-phase inflammation or energy metabolism (16, 37). A constitutively active version of CREBH (CREBH-CA), which mimics an ER stress response (16), activates the MNRR1 reporter (Fig. 3*A*). The promoter for MNRR1 harbors the conserved CREBH-binding sites (*SI Appendix*, Fig. S2*E*), which could explain the transcriptional activation of the MNRR1 reporter. The effect of CREBH-CA on MNRR1 was also evident at the protein level (Fig. 3*B*). To test for the effect of CREBH-CA on mitochondrial function, we measured cellular oxygen consumption in R1$^{+/+}$ and R1$^{-/-}$ cells expressing CREBH-CA and found increased oxygen consumption in R1$^{+/+}$ cells (Fig. 3*C*), suggesting that mitochondrial function in response to ER stress is regulated via MNRR1. Moreover, the induction of mitochondrial function by CREBH-CA observed in R1$^{+/+}$ cells was abolished in R1$^{-/-}$ cells (Fig. 3*C*). In contrast, a dominant negative version of CREBH (CREBH-DN) did not enhance mitochondrial function (*SI Appendix*, Fig. S2*F*). The effect of CREBH on MNRR1 was also evident in vivo by observing reduced levels of MNRR1 protein in CREBH-knockout (KO; CREBH$^{-/-}$) mouse livers (Fig. 3*D*).

Markers of UPR^{mt}, such as YME1L1, were also reduced in CREBH$^{-/-}$ mouse livers compared with WT mouse livers (Fig. 3*E*). Because MNRR1 expression is not tissue-specific, we were able to take advantage of a CREBH null animal model for this purpose. The connection between the ER-UPR and UPR^{mt} was emphasized by the observation that cells expressing CREBH-CA also display an increase in the levels of UPR^{mt} marker YME1L1, whereas this increase is not evident in cells expressing CREBH-DN (Fig. 3*F*). Taken together, these results suggest that UPR^{mt} is induced downstream of the ER-UPR, and that MNRR1 is required for the effect of CREBH on mitochondrial function. Finally, the connection appears to be unidirectional; although MNRR1 is required for the induction of UPR^{mt}

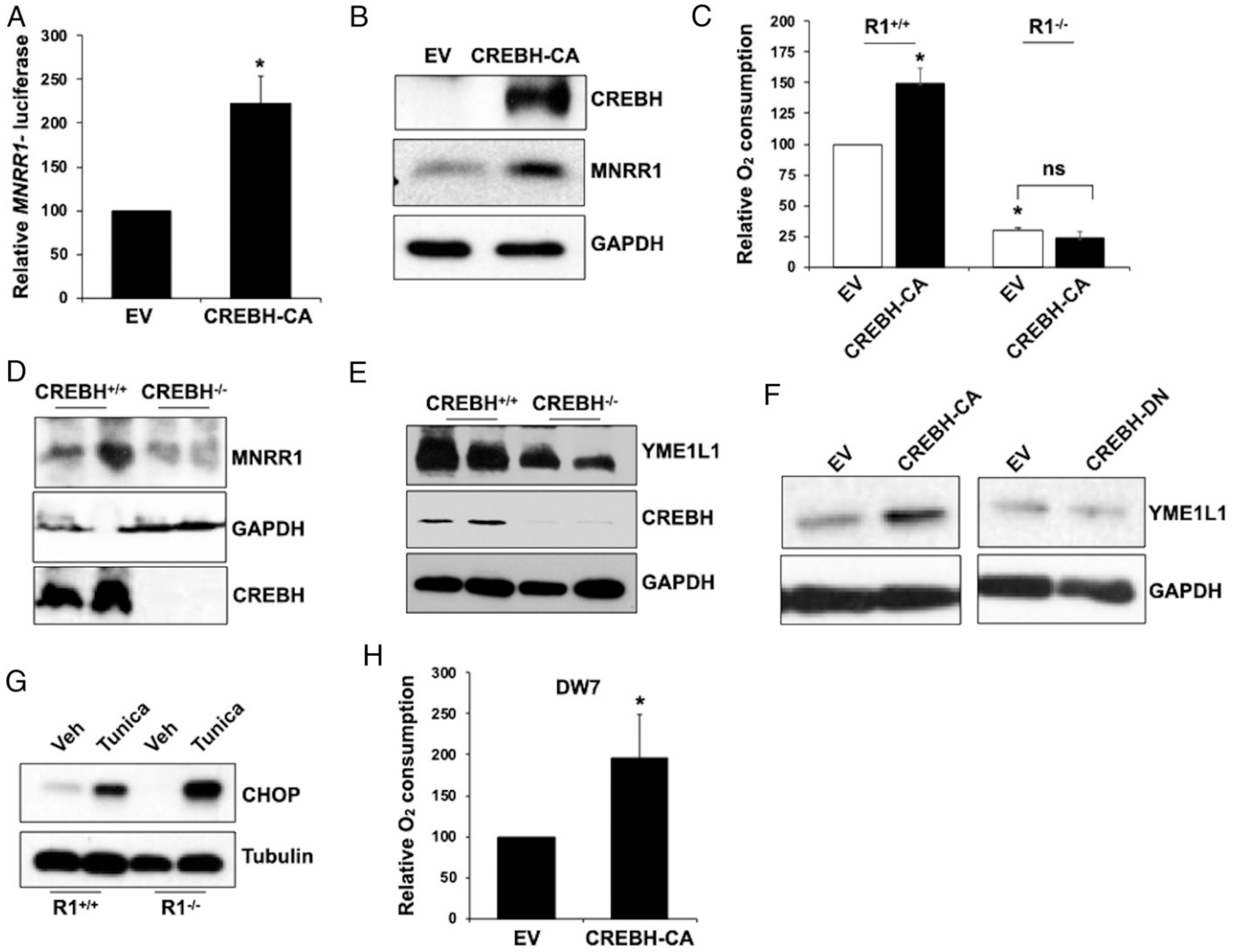

Fig. 3. CREBH, an ER stress-responsive transcription factor, activates MNRR1. (*A*) Transcription measured by a dual luciferase assay in HEK 293 cells coexpressing the MNRR1-luciferase reporter with either an EV or CREBH-CA. Data are presented as luciferase levels relative to EV-expressing cells. (*B*) MNRR1 protein levels in HEK 293 cells expressing either an EV or CREBH-CA. GAPDH served as a loading control. (*C*) Cellular oxygen consumption in intact MNRR1-KO HEK 293 cells ($R1^{-/-}$) compared with control cells ($R1^{+/+}$) expressing either an EV or CREBH-CA. Oxygen consumption is shown relative to $R1^{+/+}$ cells expressing the EV. (*D*) MNRR1 protein levels in CREBH WT ($CREBH^{+/+}$) and KO ($CREBH^{-/-}$) mouse liver tissues ($n = 2$). (*E*) UPR^{mt} marker YME1L1 protein levels in CREBH WT ($CREBH^{+/+}$) and KO ($CREBH^{-/-}$) mouse liver tissues ($n = 2$). (*F*) YME1L1 protein levels in HEK 293 cells expressing either CREBH-CA or CREBH-DN compared with cells expressing an EV. GAPDH served as a loading control. (*G*) ER stress marker CHOP protein levels in MNRR1-KO HEK 293 cells ($R1^{-/-}$) compared with control cells ($R1^{+/+}$) treated with either vehicle or 5 μg/mL tunicamycin (Tunica). (*H*) Cellular oxygen consumption in intact DW7 cells expressing either an EV or CREBH-CA. Oxygen consumption is shown relative to cells expressing the EV.

on ER stress, the induction of ER stress (by tunicamycin) does not require MNRR1 (Fig. 3*G*).

Since MNRR1 is a potential therapeutic target for the mtDNA $tRNA^{Leu(UUR)}$ m.3243A > G mutation, we sought to characterize the role of the ER stress–UPR^{mt} pathway in the MNRR1-mediated rescue of the DW7 73% m.3243A > G defect. Mitochondrial function improves on induction of the ER stress response in DW7 cells expressing CREBH-CA (Fig. 3*H*). In the DW7 MELAS cells, CREBH-CA increases MNRR1 protein levels, but CREBH-DN does not (*SI Appendix*, Fig. S3*A*).

Cellular Stress Increases Mitochondrial Turnover of MNRR1 and Inhibits Mitochondrial Import, Allowing MNRR1 Accumulation in the Nucleus. Stress has been shown to reduce mitochondrial function (38, 39), and hypoxic stress in particular has been shown to reduce mitochondrial respiration as a rescue mechanism (40). Since MNRR1 is also a hypoxia-inducible gene (2, 3), we investigated the mechanism by which MNRR1 functions under conditions of stress. MNRR1 is one of the fastest turnover proteins in the cell (41). In considering the turnover of MNRR1, given the absence of a differential ubiquitination profile between normoxic (20% oxygen) and hypoxic (4% oxygen) conditions that would suggest proteasomal degradation (*SI Appendix*, Fig. S3*B*), we decided to look at mitochondrial proteases that could be responsible for the turnover of MNRR1. YME1L1, a protease colocalized in the mitochondrial intermembrane space (IMS) (Fig. 4*A*) and induced in response to UPR^{mt}, was also found to be induced under 4% hypoxic conditions (*SI Appendix*, Fig. S2*D*).

To test whether YME1L1 is the protease responsible for MNRR1 turnover, we examined MNRR1 levels in YME1L1-KO ($Y^{-/-}$) mouse embryonic fibroblasts (MEFs) and found increased amounts compared to WT ($Y^{+/+}$) (Fig. 4*B*). Moreover, a cycloheximide chase assay confirmed increased MNRR1 stability in the $Y^{-/-}$ MEFs (Fig. 4*C*).

To test whether mitochondrial import of MNRR1 is affected under ER stress, we treated YME1L1$^{-/-}$ HEK 293 cells with tunicamycin. As shown in Fig. 4*D*, MNRR1 mitochondrial levels decrease over time, and nuclear levels increase proportionally. Since total cellular MNRR1 levels do not change (Fig. 4*D*), the data suggest diminished importation of MNRR1 into mitochondria with concurrent accumulation in the nucleus. Confocal microscopy in MEFs shows the increased localization of MNRR1 to the nucleus when cells are maintained at 4% oxygen for 8 h (Fig. 4*E*). Taken together, these results suggest that under stress, MNRR1 accumulates in the nucleus, where it can function as a transactivator to induce a transcriptional program to achieve homeostasis.

MNRR1 Expression in MELAS Cybrids Promotes Mitochondrial Biogenesis and Restores Mitophagy Markers. In addition to increasing mitochondrial respiration, expression of MNRR1 in DW7 cells increased the level of mtDNA (Fig. 5*A*). WT as well as Y99E and K-R versions of MNRR1 each increased of mtDNA levels by at least twofold, and strikingly more so for the K-R version. We generated a stable DW7 cell line expressing either an EV or WT MNRR1 to assess whether the increase in mtDNA alters its heteroplasmy. To examine whether MNRR1 expression reduced the mutant mtDNA, we exploited the HaeIII restriction site generated by the m.3243A > G mutation (*SI Appendix*, Fig. S3*C*). As shown in Fig. 5*B*, continuous MNRR1 expression reduces the level of mutant mtDNA with a concurrent greater than two fold increase in WT mtDNA level. The sequencing trace (*SI Appendix*, Fig. S3*D*) also shows an increase in WT DNA in cells expressing MNRR1. This increase in WT mtDNA ratio was seen in at least two independent clones of MNRR1. Functionally, both clones increased oxygen consumption compared with the empty vector control (*SI Appendix*, Fig. S3*E*). We considered the possibility that the perturbation caused by lentiviral transformation shifted heteroplasmy toward WT mtDNA and tested this by sequencing two independent EV control clones. We found no reduction in the percentage of mutant mtDNA in these control cells. Increased expression of TFAM (Fig. 5*C*), which is also a target of MNRR1, was consistent with TFAM's known ability to increase mtDNA copy number (42). Expression of TFAM has been previously shown to increase mtDNA copy number without an effect on biogenesis (42), and modulation of mtDNA copy number is known to rescue the phenotype of heteroplasmic mutations in mice (43). Thus, we tested whether TFAM expression could rescue the defect in MELAS cells. TFAM overexpression (*SI Appendix*, Fig. S4*A*) in DW7 cells did increase

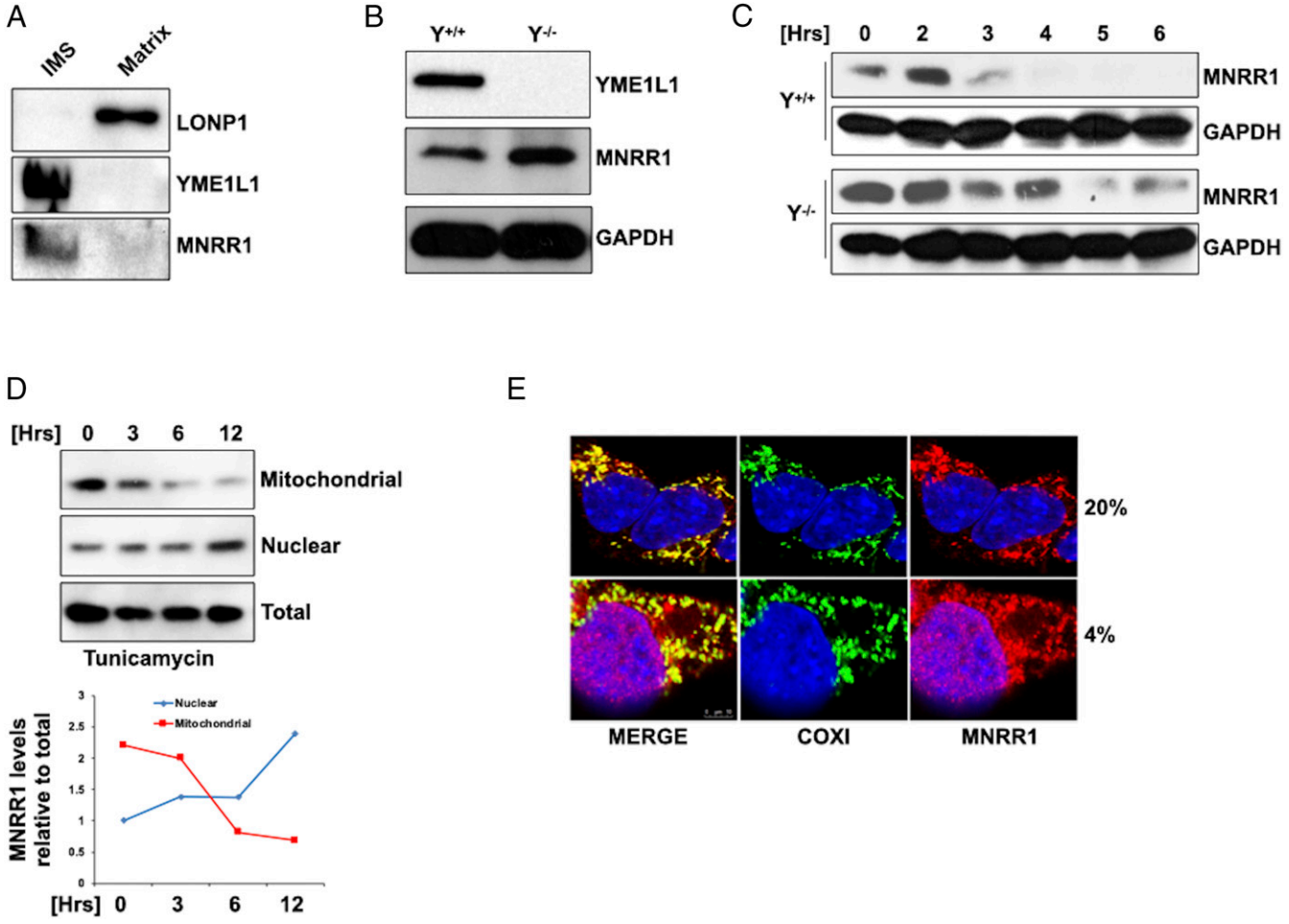

Fig. 4. Mitochondrial import of MNRR1 is inhibited under stress. (*A*) Submitochondrial localization of MNRR1 along with UPR^{mt} markers YME1L1 and LonP1. (*B*) MNRR1 levels in YME1L1-KO (Y$^{-/-}$) MEFs compared with WT (Y$^{+/+}$) cells. GAPDH served as a loading control. (*C*) Cycloheximide (CHX) chase experiment in WT (Y$^{+/+}$) and YME1L1-KO (Y$^{-/-}$) MEFs for MNRR1 levels. GAPDH served as a loading control. Cells were treated with 100 μg/mL CHX for the indicated times. (*D*) YME1L1$^{-/-}$ HEK 293 cells were treated with tunicamycin (5 μg/mL) for the indicated times. In addition to total cell lysate, treated cells were fractionated into mitochondrial and nuclear fractions, and MNRR1 levels were determined. The graph depicts the ratio of organellar fraction to total cellular MNRR1 intensity at the indicated time points. (*E*) Immunofluorescent confocal microscopy for MNRR1 localization in MEFs maintained for 8 h at either 20% or 4% oxygen. COX1 (green) was used as a mitochondrial marker, and DAPI (blue) was used to stain the nucleus. MNRR1 staining is in red.

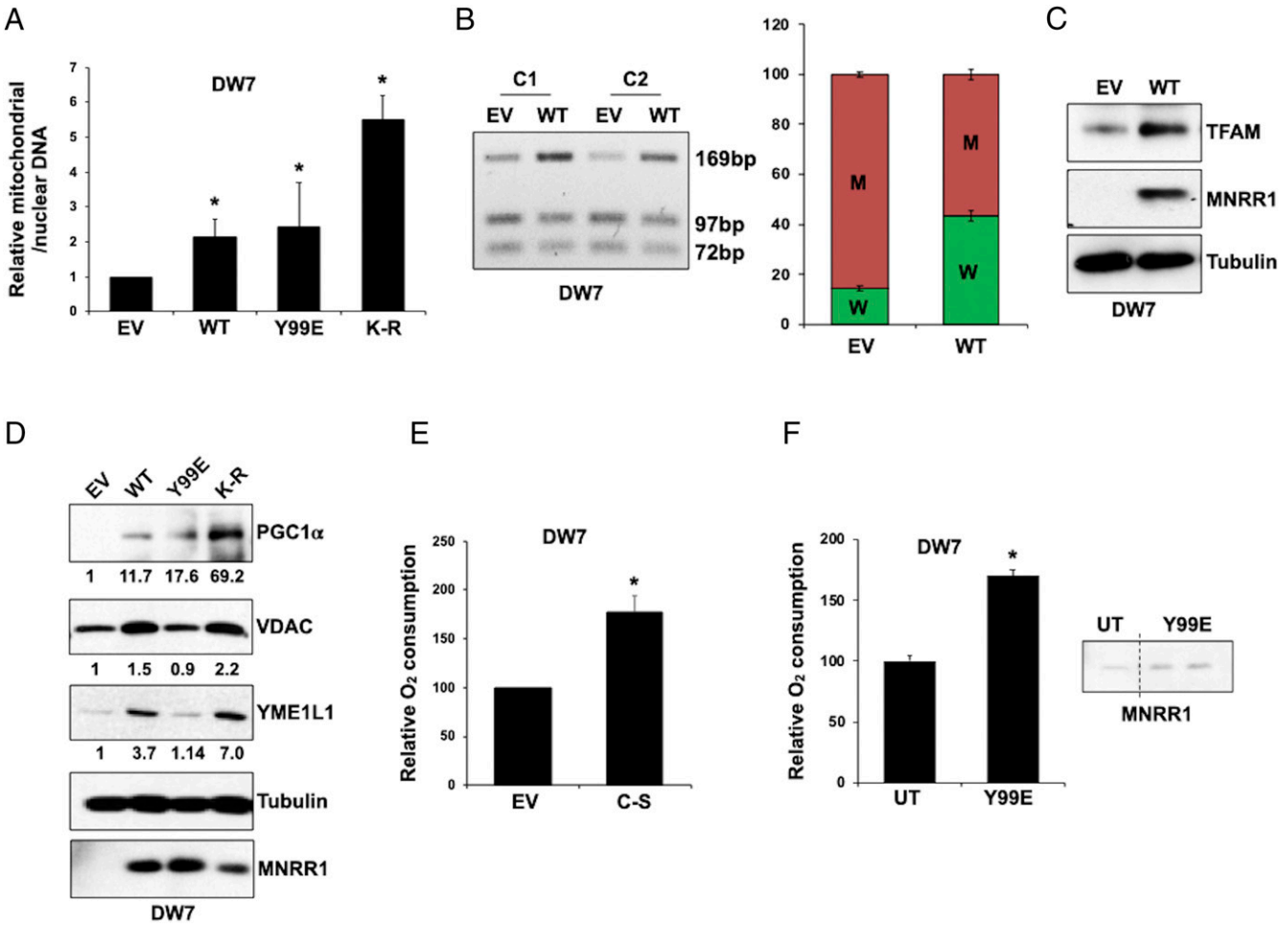

Fig. 5. Effects of MNRR1 expression in DW7 MELAS cells. (*A*) Ratio of mitochondrial DNA to nuclear DNA in DW7 MELAS cells expressing an EV, WT MNRR1, mitochondrially active (Y99E), or transcriptionally active (K-R) mutants of MNRR1. The ratio is relative to the EV value set to 1. (*B*) HaeIII restriction enzyme digestion of a PCR-amplified fragment of mtDNA harboring the 3234 mutation from DW7 cells stably expressing either an EV or WT MNRR1. Quantitation is depicted in the bar graph. W indicates WT mtDNA; M, mutant mtDNA. Two independent clones for both EV and WT (clones 1 and 2) were tested for heteroplasmy level; the bar graph shows the average of the two values. For EV, the values for clone 1 were 14.4% WT and 85.6% mutant; for WT, these values were 43.6% WT and 56.4% mutant. (*C*) WT MNRR1 expression increases TFAM levels in DW7 MELAS cells compared with those expressing the EV. (*D*) Levels of PGC1α (mitochondrial biogenesis), VDAC (mitochondrial amount), and YME1L1 (UPR^{mt}) markers in DW7 cells expressing the EV, WT MNRR1, and the mitochondrially active (Y99E) or transcriptionally active (K-R) mutants of MNRR1. Tubulin served as a loading control. Band densities relative to the EV column are shown. MNRR1 expression was detected by a Flag antibody. (*E*) Nuclear- localized mutant of MNRR1 (C-S) increases mitochondrial oxygen consumption in DW7 MELAS cells compared with the EV. (*F*) Peptide therapy rescues function in DW7 MELAS cells. (*Left*) The recombinant mitochondrially active Y99E mutant protein was transfected into DW7 MELAS cells and was able to increase mitochondrial oxygen consumption. (*Right*) Increase in MNRR1 protein in Y99E transfected cells versus nontransfected cells (UT).

mtDNA copy number (*SI Appendix*, Fig. S4*B*) but did not enhance the OCR (*SI Appendix*, Fig. S4*C*) or the level of heteroplasmy (*SI Appendix*, Fig. S4*D*), suggesting that additional pathways play roles in the rescue of the phenotype. To determine whether MNRR1 expression increases mitochondrial mass, we used protein levels of PGC-1α and VDAC as markers for mitochondrial biogenesis and found that their levels were increased in cells expressing either the WT or the K-R transcriptionally more active versions of MNRR1 but not, as expected, the mitochondrial respiration enhancing Y99E version (Fig. 5*D*). The increase in VDAC on MNRR1 expression approximately equaled the increase in mtDNA, suggesting that much of the new mtDNA arose from mitochondrial biogenesis.

The Nuclear Function of MNRR1 Is Predominantly Responsible for Restoring MELAS Cybrid Function. Since MNRR1 can act in both the nucleus and mitochondria, we sought to parse its functions by overexpressing a version of MNRR1 with C-S replacements, which cannot be imported into mitochondria but is able to function normally in the nucleus (2). We found that MNRR1-C-S is capable of rescuing respiration in DW7 cells (Fig. 5*E*), suggesting that MNRR1 induction in MELAS cells rescues the cellular bioenergetic defects. One reason for the reduced levels of MNRR1 in DW7 cells is its reduced transcription, since MNRR1 can transactivate itself (2). MNRR1-luciferase reporter levels are defective in the DW7 cells and are rescued by the introduction of the nuclear localized C-S mutant (*SI Appendix*, Fig. S4*E*) (2). The C-S mutant also increases cellular oxygen consumption in the DW7 cells, supporting the importance of the transactivation function of MNRR1 in rescuing mitochondrial function in MELAS cells. Finally, as an approach to therapeutics, we transfected recombinant Y99E protein to assess mitochondrial oxygen consumption in DW7 cells and observed increased cellular oxygen consumption (Fig. 5 *F*, *Left*) and increased MNRR1 protein (Fig. 5 *F*, *Right*).

Discussion

Our results demonstrate that increasing the expression of MNRR1 is able to rescue the cellular defects caused by the mtDNA MELAS mutation m.3243A > G by restoring respiration, reducing ROS levels, and increasing the UPR^{mt} and other proteostatic pathways. MNRR1 was previously shown to be a stress-responsive gene whose protein product acts both in mitochondria by stimulating respiration via binding to COX and in the nucleus as a transcription factor by binding to a distinct promoter element found in hundreds of genes. An important component of this rescue is increasing the mitochondria and mtDNA content, which, importantly, alters heteroplasmy by increasing the normal mtDNA fraction. An increase in mtDNA alone is expected to be important because it provides more WT mtDNA. Unless the accompanying mutant mtDNA produces a toxic gain of function, increasing WT mtDNA would provide additional energy to a cell compromised by the mutation. Several examples of this cellular strategy of increasing total amount of mtDNA containing a mixture of WT and mutant are known (43–45). However, simply increasing total mtDNA by forced expression of TFAM (*SI Appendix*, Fig. S4*A*) without changing the heteroplasmy level (*SI Appendix*, Fig. S4*D*) does not alter oxygen consumption (*SI Appendix*, Fig. S4*C*), raising the possibility that the m.3243A > G mutation gains an additional function beyond affecting protein synthesis in mitochondria. The additional effect of increasing the fraction of WT mtDNA should accelerate functional recovery. Since the increase in WT mtDNA could have involved selection for faster-growing cells, as has been postulated for the low heteroplasmy levels of the MELAS mutation in blood (46), future work will be needed to see whether MNRR1 expression can also shift heteroplasmy levels in a terminally differentiated tissue, such as muscle.

The surprising requirement for MNRR1 to trigger the UPR^{mt} led us to examine the UPR^{mt} in MELAS cells. We found a blunted response in these cells not only to triggers of the UPR^{mt}, but also to other mechanisms of damage recovery, such as mitophagy and autophagy. Thus, mitochondrial dysfunction in MELAS cells would be exacerbated by the decreased ability to selectively remove dysfunctional mitochondria. Previous studies have identified ATF5 as a mediator of the mitochondrial UPR (25). Here we show that MNRR1 appears to be upstream of ATF5 as well as of the key stress-responsive pathways mitophagy and autophagy. In addition to the protein levels (Fig. 2*D*), ATF5 transcript levels increase in the DW7 cells stably overexpressing MNRR1 (*SI Appendix*, Fig. S4*F*). Furthermore, our data also suggest that UPR^{mt} is induced by ER stress, and that this response to ER stress is dependent on MNRR1. This conclusion arises because chemical inducers of the ER stress response, such as tunicamycin and thapsigargin, induce MNRR1, as does CREBH, a well-characterized ER-resident ER stress-responsive protein (16). As demonstrated here, one target of CREBH-mediated transcriptional activation is MNRR1. The presence of CREBH upstream of MNRR1 is supported by the lower MNRR1 levels in liver tissues of CREBH-KO mice (Fig. 3*D*).

Previous work has shown enhanced mitochondrial bioenergetics during early stages of the ER stress response (13). Our results support a similar phenotype. Treatment of DW7 cells with tunicamycin increases their OCR (*SI Appendix*, Fig. S4*G*). In addition, cells expressing active CREBH display enhanced oxygen consumption. However, in the absence of MNRR1, CREBH fails to activate mitochondrial respiration, identifying MNRR1 as an indispensable stress-responsive mitochondrial regulator. The lower levels of UPR markers in MNRR1-KO cells further support this role of MNRR1. The fact that both TFAM and PGC-1α are targets of MNRR1 (Fig. 5 *C* and *D*) suggests a pathway for ER stress-mediated mitochondrial stimulation to generate energy for a stress response program and prevent apoptosis. MNRR1 has been shown to perform both these functions (2, 4).

The bi-organellar nature of MNRR1 function raises the question of which function is dominant in cellular stress recovery. Our evidence supports its nuclear function as the crucial function. Although the Y99E mutant is functionally superior in the mitochondria for oxygen consumption, it is not completely defective for its transactivation function (*SI Appendix*, Figs. S1*B* and S4*H*) and thus could partially contribute to the rescue via its

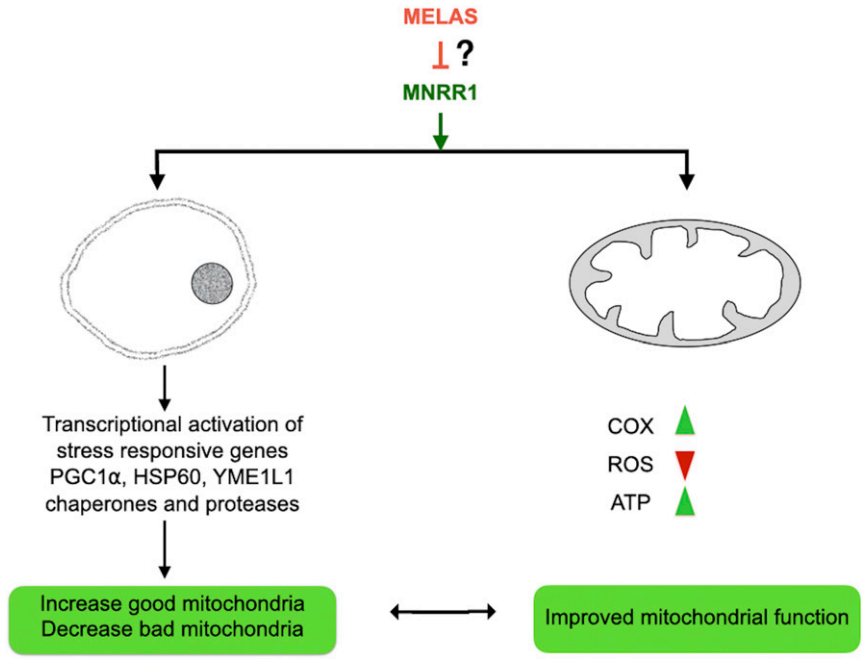

Fig. 6. Model for the mechanism of MNRR1-mediated rescue of mitochondrial function in MELAS. Via its mitochondrial function, MNRR1 increases organellar respiratory activity, and via its nuclear function, it promotes mitochondrial biogenesis and induction of quality control physiological processes, such as autophagy, to restore homeostasis.

nuclear function (Figs. 1*B* and 5 *A* and *D*). MNRR1 enters the mitochondria via the MIA40 disulfide relay (2), and, as we have previously shown, a C-S mutant does not enter mitochondria (2). Nevertheless, forced expression of the C-S mutant is able to restore respiration in these 73% m.3243A > G MELAS cybrids (Fig. 5*E*). Furthermore, expression of MNRR1 is able to increase mitochondrial mass and mtDNA (Fig. 5 *A*–*C*). Since the MNRR1 promoter itself contains the sequences to which the cognate protein binds to stimulate transcription, it provides feed-forward production of more MNRR1 protein. This parsing of organellar function could usefully constrain approaches to the therapeutic use of MNRR1.

In summary, MNRR1 rescue of MELAS cell dysfunction appears to occur through three complementary mechanisms (Fig. 6): increased mitochondrial respiration, increased total mtDNA (and possibly purifying selection of WT mtDNA), and increased pathways that turn over dysfunctional mitochondria, such as UPR^{mt}, mitophagy, and autophagy. In addition to MELAS, MNRR1 levels were also lower in 143B cells harboring the NARP (m.8993 T > G) mutation (*SI Appendix*, Fig. S2*C*). MNRR1 expression in these cells also rescued the ∼30% reduction in oxygen consumption observed in the mutant cells compared with WT controls (*SI Appendix*, Fig. S2*C*). These observations suggest that MNRR1 could be a potential target exerting broad multipathway effects in cells to rescue the phenotype; however, the safety of prolonged higher expression remains to be addressed in animal models.

Materials and Methods

Reagents.

Antibodies. Actin (catalog no. 12748), GAPDH (3683), tubulin (9099), HSP60 (46611), LC3-I/II (12741), LONP1 (56266), and PGC1α (2178) antibodies were purchased from Cell Signaling Technologies. ATG7 (catalog no. 10088-2-AP), MNRR1 (19424-1-AP and 66302-1-Ig), p62 (18420-1-AP), TFAM (19998-1-AP), VDAC (55259-1-AP), CHOP (15204-1-AP), Parkin (14060-1-AP), SIRT1 (13161-1-AP), and YME1L1 (11510-1-AP) antibodies were purchased from Proteintech. The ATF5 antibody was purchased from Santa Cruz Biotechnology (sc-377168) , and the total OxPhos mixture antibody was obtained from Abcam (ab110411). The COX1 antibody was purchased from Invitrogen (459600), and the goat anti-rabbit Alexa Fluor 594 (111-585-144) and anti-mouse secondary Alexa Fluor 488 (115-545-146) were purchased from Jackson ImmunoResearch. Flag-HPR antibody was purchased from Sigma-Aldrich (A8592). Polyclonal rabbit anti-CREBH antibody was raised by immunizing rabbits with a protein fragment spanning amino acids 75 to 250 of mouse CREBH protein (37).

Chemicals. Chemicals used in this study included doxycycline (sc-337691), paraquat (sc-257968), thapsigargin (sc-24017), tunicamycin (sc-3506), and cycloheximide (sc-3508), all from Santa Cruz Biotechnology, and brefeldin A (s7046) and SRT1720 (S1129) from Selleckchem. CM-H_2DCFDA (C6827) and MitoTracker Green (CM7514) were from Thermo Fisher Scientific. The CellTiter Glo kit (G7570) and dual luciferase reporter assay kit (E1910) were purchased from Promega.

Cell Lines. HEK 293 cells were grown in Dulbecco's modified Eagle's medium (DMEM) (HyClone, SH30243), with 10% FBS (Sigma Aldrich, F2442) and 1% penicillin-streptomycin (P/S) (Gibco, 15140-122). To generate an MNRR1 KO, HEK 293 cells were transfected with a human MNRR1 CRISPR/Cas9 KO plasmid pair (Santa Cruz Biotechnology, sc-412127 and sc-412127-HDR), followed by selection for puromycin-resistant colonies and clones. Knockout was confirmed by immunoblotting. Puromycin-resistant clones were also selected from cells transfected with an EV and used as controls for the MNRR1-KO cells. The 143B MELAS cybrid cell lines (CL9, DW10, and DW7) and NARP cells were grown in DMEM with 10% FBS, 1% P/S, 2 mM L-glutamine, 1 mM sodium pyruvate, nonessential amino acids, and 50 μg/mL uridine. YME1L1 WT and KO MEFs and HEK 293 cells were a gift from Dr. Thomas Langer, Institute of Genetics, University of Cologne. The medium for MEFs has been described previously (47). The HEK 293 YME1L1 KO cells were grown in DMEM with 10% FBS and 1% P/S. All cells were cultured in a humidified incubator at 37 °C. The normoxia-hypoxia experiments were performed as described previously (3). Liver samples used in the study from the CREBH KO ($CREBH^{-/-}$) mice with exons 4 to 7 of the *CrebH* gene deleted have been described previously (48). For stable expression of MNRR1, DW7 cells were infected with lentiviral activation particles for MNRR1 (Santa Cruz Biotechnology, sc-412127-LAC-2) according to the manufacturer's instructions. The viral particles contain three plasmids: a deactivated Cas9 (dCas9) nuclease (D10A and N863A) fused to the transactivation domain VP64, an MS2-p65-HSF1 fusion protein, and an MNRR1-specific 20-nt guide RNA. Each of the plasmids harbors a specific selection marker, puromycin, blasticidin, and hygromycin. On selection, stable clones were tested for MNRR1 expression using immunoblotting.

Plasmids. All MNRR1 expression plasmids were cloned into pCI-Neo vector with a C-terminal 3× Flag tag. The WT, Y99E, and C-S MNRR1 expression plasmids have been described previously (1, 3). The K-R MNRR1 plasmid has all three lysine residues mutated to arginines, mimicking a deacetylated protein. Similarly, K119R, K132R, and K142R have each of the individual lysine residues mutated. The K-Q mutant has all lysine residues mutated to glutamine, representing an acetylmimetic. The MNRR1-luciferase reporter plasmid and the COX4I2 luciferase reporter plasmids have been described previously (2, 3). The OTC and Δ OTC plasmids were a gift from Dr. Richard Youle, National Institute of Neurological Disorders and Stroke. The expression vector expressing CREBH-CA was constructed by inserting the sequence encoding the nuclear form of human CREBH protein (amino acids 1 to 321) into the pFlagCMV-4 plasmid vector (16). The vector expressing CREBH-DN was constructed by inserting the sequence encoding only the human CREBH protein basic leucine zipper domain (amino acids 209 to 320) into the pFlagCMV-4 vector. mCherry-Mito-7 was a gift from Michael Davidson (Addgene plasmid 55102; http://www.addgene.org/55102). The SIRT1 expression plasmid was purchased from the DNASU Plasmid Repository (clone ID HsCD00441747). The TFAM expression plasmid with a C-terminal Flag epitope was purchased from GenScript Biotech. All expression plasmids were purified using the Qiagen EndoFree plasmid purification kit.

Mitochondrial Isolation and Subfractionation. Cellular mitochondrial and nuclear fractions were isolated from cells with the Thermo Fisher Mitochondrial Isolation Kit For Cultured Cells (Thermo Fisher Scientific, 89874) according to the manufacturer's protocol. Submitochondrial fractionation was performed as described previously (49).

Coimmunoprecipitation and Immunoblotting. Coimmunoprecipitation and immunoblotting were performed as described previously using specific antibodies (1–3).

Reporter Assays. Luciferase reporter assays were performed using the dual luciferase reporter assay kit (E1960, Promega) as described previously (2, 3).

Confocal Microscopy. MEFs were grown on 12-mm coverslips in six-well plates and incubated in either 20% or 4% O_2. They were then fixed in 4% paraformaldehyde for 10 min, rinsed in PBS, processed with 10 mM citric acid and 0.1% Tween-20 (pH 6.0) for 10 min at 95 °C and then for 20 min at room temperature for antigen retrieval. Coverslips were then rinsed twice with PBS and incubated with mouse anti-COX1 (diluted 1:100) and mouse anti-MNRR1 antibody (diluted 1:50) for 1 h at room temperature, rinsed three times with PBS, and then incubated with secondary antibodies goat anti-mouse IgG Alexa Fluor 488 and goat anti-rabbit IgG Alexa Fluor 594 (1:300) for 1 h. The coverslips were then rinsed three times with PBS, and the cells were stained with DAPI. After three more washes in PBS, the coverslips were mounted with Aqua-Mount (Thermo Fisher Scientific).

Cells were imaged on a Leica TCS SP5 microscope, and images were processed in Adobe Photoshop. Colocalization was confirmed using Volocity image analysis software (PerkinElmer Life Sciences). The Pearson correlation coefficient was calculated as described previously (1).

Intact Cellular Oxygen Consumption. Cellular mitochondrial function was measured on an Agilent Seahorse XFe24 Bioanalyzer according to the manufacturer's instructions. Unless specified otherwise, 30,000 cells per well per day were plated prior to assay. Data were normalized to the protein concentration and are presented as oxygen consumption relative to the control set to 100%.

Mitochondrial DNA Levels. Total genomic DNA was isolated from cells expressing each of the mutants using the Invitrogen PureLink Genomic DNA Mini Kit (Thermo Fisher Scientific, K1820-01). Real-time PCR analysis was performed using the SYBR Green assay on an ABI 7500 PCR system (Applied Biosystems). Data were analyzed using the $\Delta\Delta^{CT}$ method. The primer sequences used to amplify mtDNA and 18s rRNA were as follows: mtDNA: forward, 5′-CCTCCCTGTACGAAAGGAC-3′; reverse, 5′- GCGATTAGAATGGGTACAATG-3′; 18s: forward, 5′-CCAGTAAGTGCGGGTCATAA-3′; reverse, 5′-GGCCTCACTAAACCATCCAA-3′.

SYBR-Green Real-Time PCR. Transcript levels of MNRR1, ATF5, and GAPDH were measured by real-time PCR using a SYBR-Green assay on an ABI 7500 system as described previously (3). Total cellular RNA was extracted using the RNeasy Plus Mini Kit (Qiagen) in accordance with the manufacturer's instructions. cDNA was generated by reverse-transcriptase PCR using the ProtoScript II First-Strand cDNA Synthesis Kit (New England BioLabs). Real-time analysis was performed by the $\Delta\Delta^{CT}$ method. Primer sequences were as follows. MNRR1: forward, 5′- CACACA TTGGGTCACGCCATTACT- 3′; reverse, 5′-TTCTGGGCACACTCCAGAAACTGT-3′; ATF5: forward, 5′-CTGGCTCCCTAT-GAGGTCCTTG-3′; reverse, 5′-GAGCTGTGA-AATCAACTCGCTCAG-3′; GAPDH: forward, 5′-GAGTCAACGGATTTGGTCGT-3′; reverse, 5′-TTGATTTTGGAGGGA-TCTCG -3′.

Restriction Enzyme Digestion. DNA was analyzed for the MELAS mutation (the A→G mutation creates a new HaeIII site at position 3243) by PCR using primers corresponding to the light-strand positions 3116 to 3134 and to the heavy-strand positions 3353 to 3333 (50). Equal amounts of the resulting products were digested with the restriction enzyme HaeIII and electrophoresed on 2.5% agarose gel. The control and MNRR1-transformed clones were assessed at the same time by both restriction digestion and DNA sequencing to avoid bias due to restriction-insensitive heteroduplexes as a result of PCR amplification.

Statistical Analysis. All statistical analyses were performed with the two-sided Wilcoxon rank sum test using MSTAT version 6.1.1 (N. Drinkwater, University of Wisconsin–Madison). $*P < 0.05$; $**P < 0.005$.

Data Availability. All study data are included in the main text and *SI Appendix*.

ACKNOWLEDGMENTS. We thank Thomas Langer (University of Cologne) for providing his YME1L1$^{-/-}$ cells and Dr. Richard Youle (NIH) for providing the OTC plasmids. This work was supported by the Office of the Assistant Secretary of Defense for Health Affairs through the Peer-Reviewed Medical Research Program under Awards W81XWH-16-1-0516 (to L.I.G.) and W81XWH-16-1-0401 (to D.C.W.); NIH Grants NS021328, MH108592, and OD010944 (to D.C.W.) and DK090313 (to K.Z.); and the Henry L. Brasza endowment at Wayne State University (to L.I.G.). The views expressed in this article are those of the authors and do not necessarily reflect the position or policy of the Department of Defense or the US Government.

1. S. Aras *et al.*, Abl2 kinase phosphorylates bi-organellar regulator MNRR1 in mitochondria, stimulating respiration. *Biochim. Biophys. Acta Mol. Cell Res.* **1864**, 440–448 (2017).
2. S. Aras *et al.*, MNRR1 (formerly CHCHD2) is a bi-organellar regulator of mitochondrial metabolism. *Mitochondrion* **20**, 43–51 (2015).
3. S. Aras *et al.*, Oxygen-dependent expression of cytochrome c oxidase subunit 4-2 gene expression is mediated by transcription factors RBPJ, CXXC5, and CHCHD2. *Nucleic Acids Res.* **41**, 2255–2266 (2013).
4. Y. Liu *et al.*, CHCHD2 inhibits apoptosis by interacting with Bcl-xL to regulate Bax activation. *Cell Death Differ.* **22**, 1035–1046 (2015).
5. D. M. Kirby *et al.*, Mutations of the mitochondrial ND1 gene as a cause of MELAS. *J. Med. Genet.* **41**, 784–789 (2004).
6. I. Pénisson-Besnier *et al.*, Recurrent brain hematomas in MELAS associated with an ND5 gene mitochondrial mutation. *Neurology* **55**, 317–318 (2000).
7. M. A. Calvaruso *et al.*, New mitochondrial tRNA HIS mutation in a family with lactic acidosis and stroke-like episodes (MELAS). *Mitochondrion* **11**, 778–782 (2011).
8. E. Ciafaloni *et al.*, Widespread tissue distribution of a tRNALeu(UUR) mutation in the mitochondrial DNA of a patient with MELAS syndrome. *Neurology* **41**, 1663–1664 (1991).
9. R. W. Taylor *et al.*, MELAS associated with a mutation in the valine transfer RNA gene of mitochondrial DNA. *Ann. Neurol.* **40**, 459–462 (1996).
10. Y. Goto, I. Nonaka, S. Horai, A mutation in the tRNA(Leu)(UUR) gene associated with the MELAS subgroup of mitochondrial encephalomyopathies. *Nature* **348**, 651–653 (1990).
11. M. Picard *et al.*, Progressive increase in mtDNA 3243A>G heteroplasmy causes abrupt transcriptional reprogramming. *Proc. Natl. Acad. Sci. U.S.A.* **111**, E4033–E4042 (2014).
12. Y. Kozutsumi, M. Segal, K. Normington, M. J. Gething, J. Sambrook, The presence of malfolded proteins in the endoplasmic reticulum signals the induction of glucose-regulated proteins. *Nature* **332**, 462–464 (1988).
13. R. Bravo *et al.*, Increased ER-mitochondrial coupling promotes mitochondrial respiration and bioenergetics during early phases of ER stress. *J. Cell Sci.* **124**, 2143–2152 (2011).
14. I. Tabas, D. Ron, Integrating the mechanisms of apoptosis induced by endoplasmic reticulum stress. *Nat. Cell Biol.* **13**, 184–190 (2011).
15. I. Kim, W. Xu, J. C. Reed, Cell death and endoplasmic reticulum stress: Disease relevance and therapeutic opportunities. *Nat. Rev. Drug Discov.* **7**, 1013–1030 (2008).
16. K. Zhang *et al.*, Endoplasmic reticulum stress activates cleavage of CREBH to induce a systemic inflammatory response. *Cell* **124**, 587–599 (2006).
17. Z. Zheng *et al.*, CREBH couples circadian clock with hepatic lipid metabolism. *Diabetes* **65**, 3369–3383 (2016).
18. H. Kim, Z. Zheng, P. D. Walker, G. Kapatos, K. Zhang, CREBH maintains circadian glucose homeostasis by regulating hepatic glycogenolysis and gluconeogenesis. *Mol. Cell. Biol.* **37**, e00048-17 (2017).
19. R. D. Martinus *et al.*, Selective induction of mitochondrial chaperones in response to loss of the mitochondrial genome. *Eur. J. Biochem.* **240**, 98–103 (1996).
20. Q. Zhao *et al.*, A mitochondrial-specific stress response in mammalian cells. *EMBO J.* **21**, 4411–4419 (2002).
21. J. E. Aldridge, T. Horibe, N. J. Hoogenraad, Discovery of genes activated by the mitochondrial unfolded protein response (mtUPR) and cognate promoter elements. *PLoS One* **2**, e874 (2007).
22. J. Durieux, S. Wolff, A. Dillin, The cell-non-autonomous nature of electron transport chain-mediated longevity. *Cell* **144**, 79–91 (2011).
23. M. W. Pellegrino *et al.*, Mitochondrial UPR-regulated innate immunity provides resistance to pathogen infection. *Nature* **516**, 414–417 (2014).
24. P. Martinelli, E. I. Rugarli, Emerging roles of mitochondrial proteases in neurodegeneration. *Biochim. Biophys. Acta* **1797**, 1–10 (2010).
25. C. J. Fiorese *et al.*, The transcription factor ATF5 mediates a mammalian mitochondrial UPR. *Curr. Biol.* **26**, 2037–2043 (2016).
26. A. M. Nargund, M. W. Pellegrino, C. J. Fiorese, B. M. Baker, C. M. Haynes, Mitochondrial import efficiency of ATFS-1 regulates mitochondrial UPR activation. *Science* **337**, 587–590 (2012).
27. N. Purandare, M. Somayajulu, M. Hüttemann, L. I. Grossman, S. Aras, The cellular stress proteins CHCHD10 and MNRR1 (CHCHD2): Partners in mitochondrial and nuclear function and dysfunction. *J. Biol. Chem.* **293**, 6517–6529 (2018).
28. S. J. Mitchell *et al.*, The SIRT1 activator SRT1720 extends lifespan and improves health of mice fed a standard diet. *Cell Rep.* **6**, 836–843 (2014).
29. I. K. Law *et al.*, Identification and characterization of proteins interacting with SIRT1 and SIRT3: Implications in the anti-aging and metabolic effects of sirtuins. *Proteomics* **9**, 2444–2456 (2009).
30. M. Chevallet *et al.*, Alterations of the mitochondrial proteome caused by the absence of mitochondrial DNA: A proteomic view. *Electrophoresis* **27**, 1574–1583 (2006).
31. S. G. Olenych, N. S. Claxton, G. K. Ottenberg, M. W. Davidson, The fluorescent protein color palette. *Curr. Protoc. Cell Biol.* **36**, 21.5.1–21.5.34 (2007).
32. V. Jovaisaite, L. Mouchiroud, J. Auwerx, The mitochondrial unfolded protein response, a conserved stress response pathway with implications in health and disease. *J. Exp. Biol.* **217**, 137–143 (2014).
33. N. Moullan *et al.*, Tetracyclines disturb mitochondrial function across eukaryotic models: A call for caution in biomedical research. *Cell Rep.* **10**, 1681–1691 (2015).
34. T. Yoneda *et al.*, Compartment-specific perturbation of protein handling activates genes encoding mitochondrial chaperones. *J. Cell Sci.* **117**, 4055–4066 (2004).
35. M. Schröder, R. J. Kaufman, ER stress and the unfolded protein response. *Mutat. Res.* **569**, 29–63 (2005).
36. J. Sakai *et al.*, Sterol-regulated release of SREBP-2 from cell membranes requires two sequential cleavages, one within a transmembrane segment. *Cell* **85**, 1037–1046 (1996).
37. H. Kim *et al.*, Liver-enriched transcription factor CREBH interacts with peroxisome proliferator-activated receptor α to regulate metabolic hormone FGF21. *Endocrinology* **155**, 769–782 (2014).
38. H. Cui, Y. Kong, H. Zhang, Oxidative stress, mitochondrial dysfunction, and aging. *J. Signal Transduct.* **2012**, 646354 (2012).
39. G. Solaini, A. Baracca, G. Lenaz, G. Sgarbi, Hypoxia and mitochondrial oxidative metabolism. *Biochim. Biophys. Acta* **1797**, 1171–1177 (2010).
40. K. Heerlein, A. Schulze, L. Hotz, P. Bärtsch, H. Mairbäurl, Hypoxia decreases cellular ATP demand and inhibits mitochondrial respiration of a549 cells. *Am. J. Respir. Cell Mol. Biol.* **32**, 44–51 (2005).
41. M. Larance, Y. Ahmad, K. J. Kirkwood, T. Ly, A. I. Lamond, Global subcellular characterization of protein degradation using quantitative proteomics. *Mol. Cell. Proteomics* **12**, 638–650 (2013).
42. M. I. Ekstrand *et al.*, Mitochondrial transcription factor A regulates mtDNA copy number in mammals. *Hum. Mol. Genet.* **13**, 935–944 (2004).
43. R. Filograna *et al.*, Modulation of mtDNA copy number ameliorates the pathological consequences of a heteroplasmic mtDNA mutation in the mouse. *Sci. Adv.* **5**, eaav9824 (2019).
44. M. Jiang *et al.*, Increased total mtDNA copy number cures male infertility despite unaltered mtDNA mutation load. *Cell Metab.* **26**, 429–436.e4 (2017).
45. C. Giordano *et al.*, Efficient mitochondrial biogenesis drives incomplete penetrance in Leber's hereditary optic neuropathy. *Brain* **137**, 335–353 (2014).
46. S. Shanske *et al.*, Varying loads of the mitochondrial DNA A3243G mutation in different tissues: Implications for diagnosis. *Am. J. Med. Genet. A.* **130A**, 134–137 (2004).
47. R. Anand *et al.*, The i-AAA protease YME1L and OMA1 cleave OPA1 to balance mitochondrial fusion and fission. *J. Cell Biol.* **204**, 919–929 (2014).
48. C. Zhang *et al.*, Endoplasmic reticulum-tethered transcription factor cAMP responsive element-binding protein, hepatocyte specific, regulates hepatic lipogenesis, fatty acid oxidation, and lipolysis upon metabolic stress in mice. *Hepatology* **55**, 1070–1082 (2012).
49. M. Darshi *et al.*, ChChd3, an inner mitochondrial membrane protein, is essential for maintaining crista integrity and mitochondrial function. *J. Biol. Chem.* **286**, 2918–2932 (2011).
50. M. P. King, Y. Koga, M. Davidson, E. A. Schon, Defects in mitochondrial protein synthesis and respiratory chain activity segregate with the tRNA(Leu(UUR)) mutation associated with mitochondrial myopathy, encephalopathy, lactic acidosis, and strokelike episodes. *Mol. Cell. Biol.* **12**, 480–490 (1992).